

Manuscript ID bg-2019-389 titled “**The influences of historic lake trophy and mixing regime changes on long-term phosphorus fractions retention in sediments of deep, eutrophic lakes: a case study from Lake Burgäschi, Switzerland**”.

We would like to thank the reviewer for the helpful comments to improve the quality of this manuscript. Our response to the reviewer follows point by point.

Reviewer concerns:

The authors have appropriately addressed all comments and suggestions. I add some minor suggestions that may help improving the text:

1. Line 13: add “... on short time scales in shallow lakes”

Response: Done, modified.

2. Line 14: replace "eutrophication" by "trophic state"

Response: Done, modified.

3. Line 15: replace "reduce" by diminish"

Response: Done, modified.

4. Line 18-19: replace “...provides information...” by “...provide information on the benthic P retention under the influence...”.

Response: Done, modified.

5. Line 21: delete “restoration”. Delete “the operation of”

Response: The two modifications are done.

6. Line 25: replace “hypolimnetic had better...” by “...sediment overlaying water was seasonally oxic”

Response: Done, replaced.

7. Line 26-27: I suggest: “...in the hypolimnion and due to hypolimnetic water withdrawal increasing the P export out of the lake, net burial rates of total and labile P fractions decreased considerably in surface sediments.”

Response: As suggested, the sentence has been modified.

8. Abstract: As you mention "mixing regime" in the title you should explain in the abstract if and how hypolimnetic withdrawal affected the general character of the mixing regime.

Response: We have added the sentence "Also, this restoration has not enhanced water-column mixing and oxygenation in hypolimnetic waters." (Line 33) to indicate that hypolimnetic withdrawal did not improve the lake vertical mixing.

9. Line 88-89: Omit sentence

Response: Done, modified.

10. Line 93: replace "has operated in the lake" by "is in operation"

Response: Done, modified.

11. Line 103: replace "agricultural lands" by "farmland"

Response: Done, modified.

12. Line 106: "The mean annual AIR temperature..."

Response: Done, it is corrected.

13. Line 115: replace "algae" by "algal".

Response: Done, modified.

14. Line 115: What does "oxygenation condition" mean in this context?

Response: We have replaced "oxygenation" into "oxic/anoxic".

15. Line 128: Does "afterwards" mean that bulk elements were determined in the remains of the sediment samples after the P extraction procedure? If not, please clarify!

Response: We apologize for the confusion. We have clarified the texts by replacing the sentence with "After sampling for P extraction, the remaining sediment of the 2-cm slice was.....". (Line 143)

16.Line 287: delete “relatively”.

Response: Done, modified.

17.Line 288: replace “during” by “within”

Response: Done, modified.

18.Line 289: delete “reduced”

Response: We have replaced “reduced” with “decreased” to clarify that the labile P fractions and TP concentrations were decreased in Zone II.

19.Line 316: replace “had” by “received”

Response: Done, modified.

20.Line 319-320: “...Lake Burgäschi was likely oligo- to mesotrophic.”

Response: Done, modified.

21.Line 331: replace “and” by “indicating”.

Response: Done, modified.

22.Line 332-333: delete “reveal strong positive trends in lake eutrophic levels. The significant eutrophication in Lake Burgäschi might have caused”

Response: Done, modified.

23.Line 334: delete “many”

Response: Done, modified.

24.Line 350: replace “during” by “in zones I to III, Mn and Fe varied mostly independent...”

Response: Done, modified.

25.Line 353: Specify: What sort of ratios?

Response: It is the ratios of Fe/Mn from XRF measurements. We have clarified it by adding “The proxy of...”. (Line 383-384)

26.Line 386: delete “completely”

Response: Done, modified.

27.Line 387: replace “circulation” by “overturn”. Delete “still”

Response: Done, modified.

28.Line 414: are retention and NBR not synonyms?

Response: They are not synonyms because they have different units. In the context, “retention” refers to the contents or the concentrations (mg/kg); but NBR is the net flux with the unit of $\mu\text{g}/(\text{cm}^2\text{-yr})$.

29.Line 457: If the epilimnion P concentrations exceed about 10 $\mu\text{g}/\text{l}$ phytoplankton growth is likely not P limited.

Response: Yes, the total P data in hypolimnion of Burgäschisee is between 10-50 $\mu\text{g}/\text{L}$ (see Figure S11 in Supplementary Online Materials) but the epilimnion is expected to have lower P concentrations, probably $< 10 \mu\text{g}/\text{L}$ sometimes.

According to the study of GBL (1995), the algae-available ortho-phosphate was almost completely used up in the epilimnion during growth season and the high nitrogen concentrations (0.5-3 mg/L) were measured at the same time. We are assuming that phytoplankton production in Burgäschisee is likely limited by phosphorus at least during growth season. We have clarified it in Line 488-490.

GBL. Burgäschisee. Resultate der Wasser- und Planktonuntersuchungen 1977-1995. Office for Water Protection and Waste Management of the Canton of Bern, 1995.

30. Line 460: “... the high lake external P load into the epilimnion...”

Response: Done, modified.

1 **The influences of historic lake trophy and mixing regime**
2 **changes on long-term phosphorus fractions retention in**
3 **sediments of deep, eutrophic lakes: a case study from Lake**
4 **Burgäschi, Switzerland**

5 Luyao Tu¹, Paul Zander¹, Sönke Szidat², Ronald Lloren^{3,4}, Martin Grosjean¹

6 ¹ Oeschger Centre for Climate Change Research and Institute of Geography, University of Bern, Switzerland

7 ² Oeschger Centre for Climate Change Research and Department of Chemistry and Biochemistry, University of Bern, Switzerland

8 ³ Department of Earth Science, ETH Zürich, Switzerland

9 ⁴ Eawag, Swiss Federal Institute of Aquatic Science and Technology, Switzerland

10 *Correspondence to:* Luyao Tu (luyao.tu@giub.unibe.ch)

11

12 **Abstract.** Hypolimnetic anoxia in eutrophic lakes can delay lake recovery to lower trophic states via the release
13 of sediment phosphorus (P) to surface waters on short time scales in shallow lakes. However, the long-term effects
14 of hypolimnetic redox conditions and trophic state on sedimentary P-fraction retention in deep lakes are not clear
15 yet. Hypolimnetic withdrawal of P-rich water is predicted to diminish sedimentary P and seasonal P recycling
16 from the lake hypolimnion. Nevertheless, there is a lack of evidence from well-dated sediment cores, in particular,
17 from deep lakes, about the long-term impact of hypolimnetic withdrawal on sedimentary P retention. In this study,
18 long-term sedimentary P-fraction data since the early 1900s from Lake Burgäschi provides information on the
19 benthic P retention, under the influence of increasing lake primary productivity (sedimentary green-pigments
20 proxy), variable hypolimnion oxygenation regimes (Fe/Mn ratio proxy), and hypolimnetic withdrawal since 1977.
21 Results show that, before hypolimnetic withdrawal (during the early 1900s to 1977), redox-sensitive Fe/Mn-P
22 fraction comprised ~50% of total P in the sediment profile. Meanwhile, long-term retention of total P and labile
23 P-fractions in sediments was predominantly affected by past hypolimnetic redox conditions, and P retention
24 increased in sedimentary Fe- and Mn enriched layers when the sediment overlaying water was seasonally oxic.
25 However, from 1977-2017, eutrophication-induced persistent anoxic conditions in the hypolimnion and due to
26 hypolimnetic water withdrawal increasing the P export out of the lake, net burial rates of total and labile P fractions
27 decreased considerably in surface sediments. By contrast, refractory Ca-P fraction retention was primarily related
28 to lake primary production. Due to the lake restoration since 1977, Ca-P fraction became the primary P fraction in
29 sediments (representing ~39% of total P), indicating a lower P bioavailability of surface sediments. Our study
30 implies that in seasonally-stratified eutrophic deep lakes (like Lake Burgäschi), hypolimnetic withdrawal can
31 effectively reduce P retention in sediments and potentials of sediment-P release (internal P loads). However, more
32 than 40 years of hypolimnetic syphoning have not improved the lake trophic state or decreased lake productivity.
33 Also, this restoration has not enhanced water-column mixing and oxygenation in hypolimnetic waters. The
34 findings of this study are relevant regarding management of deep eutrophic lakes with mixing regimes typical for
35 temperate zones.

36

37 **Keywords:** Phosphorus fractions, eutrophication, hypolimnetic anoxia, hypolimnetic withdrawal, deep lakes

38

Deleted: eutrophication

Deleted: reduce

Deleted: information on the potential availability and retention of sediment-P

Deleted: s

Deleted: restoration

Deleted: the operation of

Deleted: hypolimnetic had better seasonally oxic conditions

Deleted: nd hypolimnetic withdrawal both contributed to considerably decreased retention and net burial rates of total P and labile P fractions

50

51 **1 Introduction**

52 Phosphorus (P) eutrophication in freshwater lakes is a global problem and has been a matter of concern to the
53 public for several decades. In lakes where the external P loading has been reduced, internal P loading (sediment-
54 P release to surface waters) is widely recognized as the key factor affecting lake trophic status and delaying lake
55 recovery from eutrophication (Burley et al., 2001; Trolle et al., 2010). Considerable work has been done on
56 sediment-P speciation to evaluate sediment-P release potentials and implications for lake restoration management
57 (Gonsiorczyk et al., 1998; Ribeiro et al., 2008).

58 The paradigm that oxygen levels control the sediment-P release via reductive dissolution of Fe-P fraction in surface
59 sediments has been accepted as the classical model for a long time (Einsele, 1936, 1938; Moosmann et al., 2006).
60 Under anoxic conditions, P bound to redox-sensitive Fe and Al/Fe (oxyhydr)oxides can be potentially released
61 from surface sediments into lake water (Burley et al., 2001), which was supported by numerous short-term (days
62 or seasonal) laboratory or in-situ studies (Chen et al., 2018). Based on this paradigm, it was assumed that an oxic
63 sediment–water interface might limit the release of Fe-P from sediments and, therefore, improve P retention in
64 lake sediments. However, the restoration measures with artificial hypolimnetic oxygenation/aeration applied in
65 eutrophic lakes proved to have only short-lasting effects but no direct effects on internal P loading and redox-
66 dependent sediment-P retention on longer terms (Gächter, 1987; Gächter and Wehrli, 1998; Moosmann et al., 2006;
67 Hupfer and Lewandowski, 2008). Gächter and Müller (2003) and Moosmann et al. (2006) further argued that, on
68 multi-decadal or longer time scales, P retention in lake sediments might eventually primarily depend on the P-
69 binding capacity of anoxic sediments and sediment composition (e.g. Fe, Mn, Al, and Ca contents). Nevertheless,
70 until now, there is a lack of evidence from well-dated sediment cores, and there is still a need to know which
71 processes may have a dominant influence on sediment P-fraction retention on longer time scales (e.g., decades or
72 more). This information is crucial for predicting and, ultimately, managing sediment-P release, especially in deep
73 lakes, because hypolimnetic anoxia in deep lakes can lead to large loads of sediment-P release. In contrast to the
74 well-established studies about sediment-P speciation in shallow polymictic lakes (e.g. Kaiserli et al., 2001;
75 Søndergaard et al., 2001; Cavalcante et al., 2008), there are only a few studies available from seasonally-stratified
76 deep lakes. Furthermore, eutrophication has been demonstrated to affect sediment-P release via controlling
77 hypolimnetic anoxia and lake mixing regime in seasonally stratified deep lakes (Tu et al., 2019). It is not yet fully
78 understood whether and how lake trophic levels and hypolimnetic anoxia can influence the long-term behavior of
79 sedimentary P-fraction retention in deep lakes.

80 The restoration technique of hypolimnetic withdrawal has been frequently applied in seasonally stratified lakes in
81 Europe (Kucklantz and Hamm, 1988; Nürnberg, 2007), whereby P-enriched water from the hypolimnion is
82 discharged directly into the lake outflow. This restoration technique has been shown to efficiently reduce P
83 concentrations in lake waters (Nürnberg, 2007). Hypolimnetic withdrawal was also expected to reduce P retention
84 in sediments and seasonal P recycling from the lake hypolimnion to the upper waters, for example, in Lake Mauen,
85 a shallow, eutrophic lake (maximum depth 6.8 m; Gächter, 1976). However, there is lack of empirical evidence
86 from sedimentary P-fraction data, which provides valuable information on possible sediment-P release

87 characteristics and potentials of internal P loadings. Furthermore, for deep lakes, the long-term influence of this
88 restoration on sedimentary P release potentials is unclear.

89 The objectives of this study were to (1) explore the main factors controlling long-term changes of P-fraction
90 retention in sediments of deep lakes, (2) investigate how sediment P-fraction retention responds to changes in lake
91 eutrophication and hypolimnetic anoxia of the past prior to anthropogenic eutrophication, (3) examine the long-
92 term effects of lake hypolimnetic withdrawal restoration on sedimentary P-fraction retention in seasonally-
93 stratified deep lakes, and (4) evaluate with sediment-P data the predictions from Gächter (1976) that hypolimnetic
94 withdrawal should result in reduced total P contents in sediments and sediment-P release to lake water. To achieve
95 these objectives, we investigated short sediment cores from Lake Burgäschi, a deep and eutrophic lake on the
96 Swiss Plateau. Sedimentary green-pigments (chlorophylls and diagenetic products) inferred from hyperspectral
97 imaging (HSI) scanning and XRF-inferred Fe/Mn ratios primarily reflect lake trophic state evolution (aquatic
98 primary productivity) and hypolimnetic oxygenation, respectively. A sequential P-extraction with five P fractions
99 was performed to uncover P fractionation in sediment profiles. We combined all data to identify the dominant
100 factors responsible for temporal changes in P-fraction retention. ▼

Deleted: Changes in P-fraction records for the periods before and during the restoration were also investigated.

101 Lake Burgäschi is an excellent study site because there were substantial changes in lake trophic levels and possibly
102 lake-mixing regimes since the last century (Guthruf et al., 1999; Van Raden, 2012), and exceptionally long
103 historical and limnological survey data are available for most of the last 50 years. Hypolimnetic withdrawal
104 restoration is in operation since 1977. ▼

Deleted: has operated in the lake

105

106 2 Study site

107 Lake Burgäschi (47°10'8.5"N, 7°40'5.9"E) is a small lake located on the Swiss Plateau (Fig. 1a). It has a very
108 restricted catchment (3.2 km²). The catchment area geologically belongs to the Molasse Basin, and mostly consists
109 of carbonate-rich sandstones and mudstones (Schmid et al., 2004). The kettle hole lake was formed after the retreat
110 of the Rhone glacier (ca. 19 k yr. BP; Rey et al., 2017). Currently the maximum water depth is ~31 m, which is
111 quite deep in contrast to the small surface area of 0.21 km² (Guthruf et al., 1999). The mean retention time of the
112 lake water is ~1.4 year (Nürnberg, 1987). The lake has several small inflows in the southwest (Rey et al., 2017)
113 and one outflow in the north (Fig. 1c).

114 Since the 19th century, the lake's water level was lowered several times to create farmland, with the most recent
115 lowering (up to 2 m) during 1943-1945 (Guthruf et al., 1999). Agricultural area currently covers ~55% of the lake
116 catchment, followed by ~29% area of forests. The lake region experiences a warm humid continental climate (Dfb;
117 Köppen-Geiger classification). The mean annual air temperature is 9 °C and the warmest month is July (mean
118 temperature 19 °C).

Deleted: agricultural land

119 Lake Burgäschi has been highly productive (eutrophic to highly eutrophic state) since the 1970s with high algal-
120 biomass production and anoxic conditions in the hypolimnion (Guthruf et al., 1999, 2013). The eutrophication in
121 Lake Burgäschi has been linked to increased agricultural P inputs via drainage into the lake in the second half of
122 the 20th century (Guthruf et al., 1999). To mitigate the eutrophication, hypolimnetic withdrawal restoration has
123 been applied in Lake Burgäschi since 1977, and the lake water has been monitored twice a year for more than 30

128 years for various parameters, such as pH, oxygen content, phosphorus concentrations, phytoplankton biomass, etc.
129 Despite a sharp decline in hypolimnetic phosphorus concentrations due to the restoration, a high production of
130 ~~algal~~ biomass continues today (GSA, 2007). Additionally, hypolimnetic ~~oxic/anoxic~~ conditions and the lake
131 trophic state have been stabilized but not fundamentally improved (GBL, 1995; Guthruf et al., 2013).

Deleted: algae

Deleted: oxygenation

132

133 3 Materials and methods

134 3.1 Core collection and sampling

135 In September 2017, two 75-cm-long sediment cores (Burg17-B and Burg17-C) were retrieved from the deepest
136 point of Lake Burgäschli (water depth ~31 m) (47°10'8.6"N, 07°40'5.3"E; coring site in Fig. 1c) using a UWITEC
137 gravity corer. After the collection, the cores were stored in a dark cold room (~4 °C). After opening and splitting
138 lengthwise, core-half A of Burg17-B was continuously subsampled at 2-cm resolution from 0 to 60 cm for ²¹⁰Pb
139 and ¹³⁷Cs dating. The oxidized surface of core-half B (Burg17-B) was visually described (Schnurrenberger et al.,
140 2003) before non-destructive XRF core and HSI scanning. After the opening, one-half of core Burg17-C was
141 transferred immediately into a glove box with an anoxic atmosphere where it was continuously subsampled at 2-
142 cm resolution from 0 to 72 cm. The fresh sediments from each sample slice were homogenized and used for
143 sequential P extraction. After ~~sampling for P extraction~~, the remaining sediment ~~of the 2-cm slice~~ was freeze-dried
144 and homogenized for bulk element analyses.

Deleted: wards

145 3.2 Chronology

146 The chronology of the core Burg17-B is based on ²¹⁰Pb and ¹³⁷Cs activity profiles. The freeze-dried and
147 homogeneous samples were stored dry and dark until analysis. The ²¹⁰Pb, ¹³⁷Cs and ²²⁶Ra radiometric activities
148 were measured by gamma spectrometry at the University of Bern Department of Chemistry and Biochemistry.
149 1.3-5.1 g of the freeze-dried samples were encapsulated into polystyrene petri dishes (68 mm O.D., 11 mm height;
150 Semadeni, Ostermundigen, Switzerland) together with a polystyrene disk to fill in the headspace above the sample
151 material, and the petri dishes were vacuum-sealed into a gas-tight aluminum foil for equilibration. ²¹⁰Pb (46.5 keV),
152 ²⁴¹Am (59.5 keV), ²²⁶Ra progenies ²¹⁴Pb and ²¹⁴Bi (295.2, 351.9 and 609.3 keV), as well as ¹³⁷Cs (661.7 keV) were
153 measured using a Broad Energy Germanium (BEGe) detector (Canberra GmbH, Rüsselsheim, Germany). This
154 system is composed of a high-purity germanium crystal of 50 cm² area and 30 mm thickness with a 0.6 mm thick
155 carbon epoxy window, which shows high absolute full-energy peak efficiencies for close on-top geometries of >20%
156 and ~5% for ²¹⁰Pb and ¹³⁷Cs, respectively. Low integrated background count rates of 0.20 s⁻¹ (energy range of 30-
157 1800 keV) were achieved by application of low-background materials, installation in third underground floor (~10
158 m of water-equivalent overburden), passive shielding (outside to inside: 10 cm low-background lead, 3 mm ancient
159 lead with negligible ²¹⁰Pb content, 2 mm cadmium), flushing of the shield interior with nitrogen gas and an active
160 anti-cosmic shield (plastic scintillator panels of totally 1 m² area mounted directly above the passive shielding).
161 Supported ²¹⁰Pb in each sample was assumed to be in equilibrium with the in-situ ²²⁶Ra (equilibration time 4
162 weeks). Unsupported ²¹⁰Pb activity was calculated by subtracting ²²⁶Ra activity from total ²¹⁰Pb activity level-by-
163 level. The correction for the total unsupported ²¹⁰Pb missing inventory followed Tylmann et al. (2016).

164

168 The ²¹⁰Pb chronology of core Burg17-B was determined using the Constant Rate of Supply (CRS) model (Appleby,
169 2002), which accounts for variation in sediment accumulation rates. We tested two CRS models: CRS-1 model
170 was unconstrained (i.e. without reference points from the ¹³⁷Cs activity). The CRS-2 model was constrained with
171 the chronologic marker of peak fallout from nuclear weapons testing in 1963 (¹³⁷Cs and ²⁴¹Am). Both models were
172 then tested and validated with independent time-markers at the onset of nuclear weapons testing in 1953/54 and
173 the Chernobyl accident in 1986/87 (onset of ¹³⁷Cs and peak of ¹³⁷Cs and ²⁴¹Am, respectively).

174
175 The two sediment cores (Burg 17-B and Burg 17-C) are visually very similar but show a length-offset due to coring
176 compaction of approximately 2-6 cm (Fig. S1 in Supplementary data). The age-depth stratigraphy of Burg17-C
177 core was inferred from the dated core Burg17-B by visual stratigraphic correlation from high-resolution core
178 pictures.

179

180 3.3 Non-destructive geochemical methods

181 Non-destructive X-ray fluorescence (XRF) core scanning was done using an Avaatech XRF Core Scanner (Richter
182 et al., 2006) for semi-quantitative element composition measurements at 0.5 mm resolution to capture relative
183 elemental concentrations of the laminae. The core surface was smoothed and covered with a 4- μ m-thick Ultralene
184 foil prior to the analysis. Elements were measured using a Rhodium anode and a 25 μ m Be window. The lighter
185 elements (e.g. Al, Si, P etc.) were measured for 15 seconds count time at 10 kV with 1500 A, no filter; while the
186 heavier elements (e.g. Mn, Fe, Br etc.) were exposed for 40 seconds at 30 kV with 2000 A, Pd-thin filter. Element
187 intensities (semi-quantitative concentrations) of the selected elements (Mg, Si, Al, K, Ti, Rb, P, Fe, Mn, Ca) are
188 expressed as count rates (counts per second, cps).

189 Following the methodology in Butz et al. (2015), hyperspectral imaging (HSI) scanning was performed using a
190 Specim Ltd. Single Core Scanner equipped with a visual to near infrared range (VNIR, 400–1000 nm)
191 hyperspectral linescan camera (Specim PFD-CL-65-V10E). Parameters were set for a spatial resolution of ~70
192 μ m/pixel and a spectral sampling of 1.57 nm (binning of 2). Spectral endmembers were determined using the
193 “Spectral Hourglass Wizard” of the ENVI 5.5 software package (Exelisvis ENVI, Boulder, Colorado). The relative
194 absorption band depth (RABD) index calculation was performed following the method in Schneider et al. (2018).
195 However, based on the spectral end members (Fig. S2), we used the absorption feature between the wavelengths
196 R590 and R765 (590-765 nm), i.e. RABD₅₉₀₋₇₆₅. Butz et al. (2017) and Schneider et al. (2018) revealed that this
197 index is well calibrated to absolute green-pigments (chlorophyll *a* + pheophytin *a*) concentrations in sediments.
198 The sediments in Lake Burgäschi are mostly laminated and organic-rich (Van Raden, 2012), which indicates that
199 the sediments are anoxic, bioturbation is absent, and sedimentary pigments are well-preserved (Reuss et al., 2005).
200 Therefore, in our study, the relative concentrations of green-pigments inferred from RABD₅₉₀₋₇₆₅ index values
201 provide a semi-quantitative reconstruction of lake primary productivity (total algal abundance) at sub-annual
202 resolution, and are suggested to reflect the trophic state evolution of Lake Burgäschi.

203 3.4 Phosphorus fractionation scheme and bulk elements analyses

204 The P-fractionation extraction protocol (Fig. S3) principally follows the four-step extraction protocol in Tu et al.,
205 (2019). In addition, we added the last extraction step from Lukkari et al. (2007) to determine refractory organic P

206 (F5). This P fraction (F5) is practically biologically unavailable and subject to permanent P burial. The first four
207 fractions are NaCl-TP (F1: loosely bound P), NaBD-TP (F2: redox-sensitive Fe- and Mn-bound P), NaOH-TP (F3:
208 Al- and Fe-bound P), and HCl-TP (F4: Ca-bound P) (Tu et al., 2019), whereby NaCl-TP, NaBD-TP and NaOH-
209 TP fractions together ~~are considered as~~ relatively labile P fractions because they may release P back to the water
210 column under anoxic or high pH environments (Rydin, 2000). The HCl-TP and refractory organic P (Ref.-P_o)
211 fractions are classified as relatively stable or refractory P fractions. Total P in sediments was obtained from the
212 sum of the five P fractions. The P in extract samples was measured by inductively coupled plasma mass
213 spectroscopy (7700× ICP-MS) (Agilent Technologies, Germany) after the dilution with nitric acid (HNO₃) to reach
214 a final concentration of 1% v/v HNO₃.

215 Concentrations of total carbon (TC), total nitrogen (TN), and total sulfur (S) in sediment samples were determined
216 using an Elementar vario EL Cube elemental analyzer. Total inorganic carbon (TIC) content was calculated by
217 multiplying loss on ignition at 950 °C (LOI₉₅₀, following the method proposed by Heiri et al. (2001)) by 0.273, i.e.
218 the ratio of the molecular weight of C and CO₂. Total organic carbon (TOC) content was calculated using the
219 equation TOC =TC-TIC. Sediment dry bulk density and water content were determined using wet mass (g), dry
220 mass (g) and wet volume (cm³) following the method in Håkanson and Jansson (2002).

221

222 3.5 Data analyses

223 Multivariate statistical analyses were performed with R version 3.4.2 (R Development Core Team, 2017). Prior to
224 data analyses, RABD₅₉₀₋₇₆₅ index values (resolution 70 μm) were aggregated to a spatial resolution of 0.5 mm (the
225 spatial resolution of XRF data). Stratigraphically constrained incremental sum of squares clustering (CONISS;
226 Grimm, 1987) was then performed on semi-quantitative proxies (i.e. RABD₅₉₀₋₇₆₅ index and XRF-element data)
227 with R-package “rioja” (Juggins, 2017). The number of significant clusters was determined with a broken-stick
228 test (Bennett, 1996). A principal components analysis (PCA) was performed on the centered and standardized data
229 of semi-quantitative proxies, using the “Vegan” package (Oksanen et al., 2013). XRF-element and RABD₅₉₀₋₇₆₅
230 index values were averaged within the depth range of each sample taken from core Burg17-C for P fractions. In
231 order to identify the primary factors influencing the variations in sedimentary P fractions, a redundancy analysis
232 (RDA) was performed on the centered and standardized dataset of P fractions (response variables) and other
233 sediment geochemical parameters (explanatory variables) with the “vegan” package. In the RDA computation, the
234 correlation matrix option was selected and the scaling was conducted on a correlation biplot.

235 4 Results

236 4.1 ¹³⁷Cs and ²¹⁰Pb chronology

237 The two distinctive peaks of ¹³⁷Cs in sediment profiles are detected at 31 cm and 15 cm depths (Fig. 2b),
238 corresponding to the 1963 and 1986 major fallout events, respectively (Appleby, 2002). Furthermore, ²⁴¹Am
239 activity peaks at the same depths (Fig. 2b) confirm that the 1963 and 1986 ¹³⁷Cs peaks were due to atmospheric
240 fallouts (Michel et al., 2001). The first traces of ¹³⁷Cs occur at 37 cm depth, indicating the first widely detectable
241 fallout from atmospheric nuclear testing in 1953/1954 (Pennington et al., 1973).

Deleted: as

243 The ^{210}Pb activity in core Burg17-B shows a relatively monotonic decrease down to a sediment depth of 17 cm.
244 Further down, larger variations are found (Fig. 2a). The ^{210}Pb and ^{226}Ra activities do not reach equilibrium;
245 unsupported ^{210}Pb activity in the oldest sample (59 cm) is still above the limit of detection ($14.0 \pm 6.8 \text{ Bq} \cdot \text{kg}^{-1}$). The
246 observed cumulative inventory of unsupported ^{210}Pb is $2941 \text{ Bq} \cdot \text{m}^{-2}$. We corrected this value (missing inventory
247 correction; Tylmann et al., 2016) by applying an exponential equation using the lowermost values of cumulative
248 dry mass and unsupported ^{210}Pb activity between 8 and 60 cm depths. As a result, a correction value of 125.2
249 $\text{Bq} \cdot \text{m}^{-2}$ (missing inventory) is added to the final total unsupported ^{210}Pb inventory ($3066 \text{ Bq} \cdot \text{m}^{-2}$).

250 The CRS-2 model (constrained through 1963) shows a better agreement with the independent ^{137}Cs markers at
251 1953/54 and 1986/87 than the CRS-1 model (Fig. 2c). Therefore, CRS-2 model results were chosen for determining
252 the age-depth profile and sediment mass accumulation rates (MAR) of core Burg17-B. The mean age at 59 cm
253 sediment depth dates back to ~ 1930 . The extrapolated mean age at 61 cm depth is ~ 1926 calculated using the mean
254 sediment accumulation rate between 54-60 cm ($2 \text{ yr} \cdot \text{cm}^{-1}$).

255 4.2 Sediment lithology, green-pigments (RABD₅₉₀₋₇₆₅ index) and XRF-element records

256 Four sediment facies (I to IV, Fig. 3 and 4a) are identified based on visual classification and the CONISS-analysis
257 results of XRF-element intensities.

258

259 In Zone I (75.4-61cm, pre ~ 1926), the sediments consist of visible thin brown-to-reddish laminae (Mn- and Fe
260 rich). Green-pigment concentrations inferred from RABD₅₉₀₋₇₆₅ index values show a homogenous distribution with
261 the lowest values within the sediment profile (Fig. 4d). Fe/Mn ratios vary within very low values (mostly below
262 10). The Mn, Fe, P and Fe/Ti values show high levels with large variability. Extremely low Ca amounts are noted
263 in this zone.

264

265 In Zone II (61-34cm, ~ 1926 -1960), the sediments are dark gyttja, partly laminated with light Ca-rich layers. Green-
266 pigment concentrations slightly increase yet still show little variability. A sharp increase of green-pigments
267 concentrations occurs at 60 cm, and the first two local peaks near 55 cm (~ 1938) and 48 cm (1945) are notable.
268 Fe/Mn ratios remain at slightly higher values than in Zone I. The Mn, Fe, P contents and Fe/Ti values all decline
269 to low levels and remain relatively stable. Ca counts increase gradually over the whole Zone II.

270

271 In Zone III (34-21.5 cm, ~ 1960 -1977), the sediments are mostly characterized by brown-to-reddish laminations
272 (Mn-Fe rich), with thicker and more distinct laminae contacts than in Zone I. Green-pigment concentrations exhibit
273 much higher values with positive trends, intensified variability, and several maxima (seasonal algal blooms).
274 Fe/Mn ratios first drop in the lower part (34-27 cm) and then continue to increase upward to the top-part of Zone
275 III. Fe, Mn, P, and Fe/Ti values show generally opposing trends to Fe/Mn ratios. Ca contents are elevated during
276 this period relative to Zones I and II.

277

278 In Zone IV (21.5-0 cm, ~ 1977 -2017), the sediments exhibit a clear laminated structure with much more
279 pronounced light calcite layers. The laminations are characterized by a regular succession of light calcite layers
280 (Ca-rich) and dark organic-rich layers (Fig. S4). Green-pigment concentrations display the highest levels with
281 large fluctuations, and reach distinct local maxima at 18 cm (1981), 15 cm (1985), 13 cm (1987), 12 cm (1988),

282 and 8 cm (1997) depths (Fig. 4d). Fe/Mn ratios are at similarly high values as in Zone II, yet with more variability.
283 The Fe, Mn, and P element counts and Fe/Ti all show constantly very low values. The Ca amounts are the highest
284 in the profile and show considerable variability.

285
286 Two principle components, PC1 and PC2 were shown to be significant using a broken stick model. They explain
287 ~35 % and ~30 % of the total variance in the dataset, respectively (PCA-biplot; Fig. S5). The PC1 has strong
288 positive loadings for the terrigenous elements (K, Ti, Rb etc.; Fig. 3 and S6) and thus represents mainly erosional
289 processes related to allochthonous inputs. The PC2 has strong positive loadings for redox-sensitive elements (Fe,
290 Mn), P and Fe/Ti, but negative loadings for Ca, Fe/Mn ratios and green-pigments index values. Therefore, PC2
291 reflects changes in redox conditions of hypolimnetic water and lake primary productivity. The results of additional
292 PCA analyses zone by zone (Fig. S7b) show that Mn, Fe and P were mostly independent of terrigenous elements
293 (in Zones I to III), however in Zone IV, Mn, Fe and P become correlated with the terrigenous elements. The vertical
294 profile of XRF-P matches very well with the changes of total P concentrations in sediments (Fig. S8). It reveals
295 that XRF-P data can reliably represent qualitative variations of total P concentrations in sediment profiles of Lake
296 Burgäschi.
297

298 4.3 Bulk elements and P fractions in sediment profiles

299 Sediment TIC, TOC, TOC/TN ratio, S and P fractions also show distinctive features along the four stratigraphic
300 zones (Fig. 5). From the upper part of Zone I (65.2-61 cm; ~1926) to Zone IV, TIC shows a similar pattern to the
301 XRF-Ca contents (Fig. 3 and 5) suggesting that TIC is mostly present in the form of CaCO₃. Over the whole profile,
302 TOC/TN ratios are within the range of 9-11. TOC and TOC/TN ratios exhibit mostly similar patterns from Zone I
303 to Zone III. By contrast, total sulfur (S) contents display a different pattern, showing very low values in Zone I
304 and II (mean ~0.5%), and a substantial increase in Zone III and IV.

305
306 The concentrations of labile P fractions (i.e. NaCl-TP, NaBD-TP and NaOH-TP) and total P have a similar trend
307 over the whole profile (Fig. 5 and 6a). They all display rather large values within the upper part of Zone I and
308 generally decreased values in Zone II. In Zone III, the values increase to peaks at ~25 cm depth but sharply decrease
309 to the lowest values in the upper boundary of Zone III and throughout Zone IV. HCl-TP and Ref.-P_o fractions vary
310 differently compared with the other fractions. Low contents of HCl-TP fraction are observed in Zone I and II. HCl-
311 TP fraction has a rather similar pattern as labile P fractions in Zone III, but then it remains at high levels in Zone
312 IV. Ref.-P_o fraction contents show relatively stable values from Zone I to Zone II, followed by a gradual rise in
313 Zone III and in the upper part of Zone IV. The net burial rates (NBR) of P-fraction since 1934 (Fig. S9) show
314 similar trends to the P-fraction concentrations (Fig. 5) (because sedimentation rates MAR are rather constant in
315 core Burg17-C; Fig S9), except for the Ca-P and Ref.-P_o fractions with decreasing NBR throughout the Zone IV.

316
317 Regarding the P composition in sediment profiles (Fig. 6, absolute and relative amounts), from Zone I to Zone III
318 (65.2-21.5 cm) NaBD-TP fraction is the most important P-form representing ~50% of total P followed by NaOH-
319 TP fraction. However, in Zone IV (depth above ~ 21.5 cm), HCl-TP becomes the main P fraction (~39% of total
320 P) over NaBD-TP (~30% of total P).

Deleted: relatively

Deleted: during

Deleted: reduced

324

325 The relationships between response variables and explanatory variables are visible on the redundancy analysis
326 (RDA) biplot (Fig. 7), which, in most cases, correspond well to the results of Spearman rank correlation test (Fig.
327 S10). The relatively labile P fractions (NaCl-TP, NaBD-TP and NaOH-TP) and total P in sediments are strongly
328 positively correlated with redox-sensitive elements (Fe and Mn) and autochthonous Fe (Fe/Ti). However, these P
329 fractions are negatively related to hypolimnetic oxygenation proxy (Fe/Mn ratios) and, to some extent, to lake
330 productivity indicators (green-pigments, XRF-Ca and TIC). HCl-TP and Ref.-P_o fractions are positively correlated.
331 However, only HCl-TP fraction has close positive relationships with lake productivity indicators.

332 5 Discussion

333 5.1 Trophic state evolution of Lake Burgäschi

334 Four main phases of different lake trophic levels (based on RABD₅₉₀₋₇₆₅ index values) were distinguished since the
335 early 1900s, as summarized in Fig. 8 and Fig. S11. During the period prior to ~1926 in Zone I, the lowest green-
336 pigments index values reflect low lake primary productivity. In the early 1900s, agricultural impacts around the
337 catchment area of Lake Burgäschi were not prominent (Guthruf et al., 1999). It can be expected that the lake
338 ~~received~~ low nutrient loads from the catchment drainage during this period. Lake Burgäschi is classified as
339 naturally oligotrophic based on morphometric parameters (LAWA, 1998) and as naturally mesotrophic according
340 to Binderheim-Bankay (1998). Therefore, at the times of Zone I, Lake Burgäschi was likely ~~oligo- to mesotrophic~~,

341
342 The transition to Zone II (~1926-1960) was marked by generally increased sedimentary green-pigment
343 concentrations and CaCO₃ contents (Fig. 3, 4d and 5), respectively, indicating enhanced lake primary productivity.
344 The slightly decreased TOC/TN ratio also suggests a rise in autochthonous organic matter proportion (Meyers and
345 Ishiwatari, 1993). The first two algal blooms (peaks of green-pigments index; Fig. 4d) imply a very likely
346 mesotrophic to eutrophic state of the lake. Indeed, the study of Büren (1949) revealed that in 1943-1945, the trophic
347 state of Lake Burgäschi had already shifted between mesotrophic and eutrophic. Interestingly, the water-table
348 lowering during 1943-1945 (Guthruff et al., 1999) with related enhanced drainage of intensive agricultural fields
349 and meadows (Büren, 1949) did not seem to have had an immediate impact on lake primary productivity (Fig. 3).

350
351 In Zone III (~1960-1977), continuously increasing green-pigment concentrations ~~indicating~~ several algal bloom
352 events ~~and~~ intensified CaCO₃ precipitation (TIC) and sulfur (S) contents in sediments (Fig. 4a and 5) ~~are~~ in
353 agreement with the findings from other eutrophic lakes (Holmer and Storkholm, 2001; Bonk et al., 2016; Schneider
354 et al., 2018).

355
356 During Zone IV (1977-2017), we interpret that Lake Burgäschi was in highly eutrophic conditions, based on
357 constantly high green-pigments index values and multiple prominent algal blooms (Fig. 3). Low and decreasing
358 TOC/TN ratio values (< 10) in this zone suggest a dominant source of organic matter in sediments from aquatic
359 primary production, which has been interpreted as a signal of eutrophic waters (Enters et al., 2006). Our
360 interpretation is further supported by high chlorophyll-*a* concentrations in surface waters (>8 ug L⁻¹; GSA, 2007)

Deleted: had

Deleted: i

Deleted: n low trophic levels with a possible oligotrophic-mesotrophic condition

Deleted: and

Deleted:

Deleted: reveal strong positive trends in lake eutrophic levels. The significant eutrophication in Lake Burgäschi might have caused i

Deleted: , which is

Deleted: many

372 and the dominance of blue-green algae in the phytoplankton biomass during 1977 to 1992, which characterized
373 Lake Burgäschi as highly eutrophic (GBL, 1995; Guthruf et al., 2013).

374 5.2 Reconstruction of hypolimnetic oxygenation regimes of Lake Burgäschi

375 A large number of studies have used the proxy of Fe/Mn ratios in sediments to reconstruct past water oxygenation
376 and mixing regimes of the lake, such as Mackereth (1966), Frugone-Álvarez et al. (2017), and Żarczyński et al.
377 (2019) etc. However, this proxy and its interpretation are limited to cases in which the annual cycle of Fe and Mn
378 deposition in lakes is mostly driven by redox changes in the hypolimnion and related diagenetic processes in
379 surface sediments instead of driven by terrestrial inputs (Boyle, 2001; Naeher et al., 2013). In Lake Burgäschi, in
380 Zone I to III, Mn and Fe varied mostly independently of erosion indicators as shown in Fig. S7b. Furthermore,
381 Van Raden (2012) has revealed that the presence of Mn-rich laminae in sediments of Lake Burgäschi can indicate
382 frequent short-term wind-induced mixing events in the lake. Therefore, we suggest that the deposition of Fe and
383 Mn during these three zones was mainly controlled by in-lake processes. The proxy of XRF-inferred Fe/Mn ratios
384 together with Mn precipitation in sediments reliably tracks past changes of hypolimnetic oxygenation of Lake
385 Burgäschi.

Deleted: during

Deleted: were

386 In Zone I (pre ~1926), the sediments feature well-preserved Mn-Fe rich laminations and very low Fe/Mn ratios
387 (Fig. 3 and 4a), suggesting that the lake hypolimnion was seasonally well-oxygenated. The similar occurrence of
388 visible Mn-and Fe rich laminae in sediments were also reported by Rey et al. (2017) in Lake Burgäschi and from
389 other lakes, for example, Lake of the Clouds in the US (Anthony, 1977), Lake Cadagno in the Swiss Alps (Wirth
390 et al., 2013), and Lake Żabińskie in Poland (Żarczyński et al., 2018). They revealed that the red-orange Mn-rich
391 layers mostly consist of authigenic rhodochrosite (MnCO₃) that was formed when Mn-rich anoxic bottom waters
392 are mixed with oxygenated surface waters for short intervals. The preservation of this Mn-rich layer is only
393 possible when its sedimentation process exceeds the release process under anoxic hypolimnetic conditions
394 (Stevens et al., 2000). Therefore, during this period, short-term mixing events and associated oxygenation may
395 have occurred during overall stratified or anoxic conditions in the hypolimnion.

396
397 In Zone II (~1926-1960), the higher Fe/Mn ratios and very low Mn- and autochthonous Fe (Fe/Ti) amounts are
398 interpreted as the results of stable anoxic hypolimnetic waters. The formation and preservation of Fe-and Mn-
399 oxides in sediments is largely prevented under long-term stratification/reducing conditions (Stevens et al., 2000).
400 The lake most likely developed anoxic hypolimnetic conditions with yearly incomplete or missing circulation in
401 the hypolimnion.

402
403 In Zone III (1960-1977), overall decreased Fe/Mn ratios combined with reappearing Mn-and Fe-rich laminations
404 reflect better short-term oxic conditions in hypolimnetic waters than in Zone II. However, during ~1970 to 1977,
405 Fe/Mn ratios gradually increased (Fig. 3), which points to less oxic conditions in the hypolimnion. It seems to be
406 related to synchronously progressive lake eutrophication (see Sect. 5.1). Higher primary productivity and
407 strengthened anoxia in the hypolimnion are commonly observed in stratified lakes (Giguët-Covex et al., 2010;
408 Mikomägi et al., 2016). Higher lake primary productivity increases high-rate aerobic degradation of organic matter
409 and, consequently, oxygen-depletion in the hypolimnion and sediments (Gächter and Müller, 2003; Nürnberg,
410 2007).

413

414 Finally, in Zone IV (1977- 2017) Fe/Mn ratios proxy is no longer valid to indicate hypolimnetic oxygenation
415 regime, as suggested by predominantly terrestrial sources of sediment Fe and Mn (Fig. S7b). Nevertheless, the
416 well-preserved laminated sediments during this period are a clear sign of absent benthic bioturbation and thus
417 represent an indicator of generally strong anoxic conditions in hypolimnetic waters, occurring simultaneously with
418 a highly eutrophic period. According to the limnological monitoring data of Lake Burgäschi between 1978 and
419 2007 (GSA, 2007), the lake water was ~~anoxic~~ at depths below 20 m during the summer-autumn stratification, even
420 during winter ~~overturn~~ of most years, the lake water was ~~not~~ completely mixed.

421

Deleted: completely

Deleted: circulation

Deleted: still

422 5.3 Phosphorus composition and factors controlling long-term P-fraction retention in sediments

423 Prior to 1977 (i.e. Zones I-III), NaBD-TP (redox-sensitive Fe- and Mn bound P) and NaOH-TP (partly non-
424 reducible Fe oxides-P) fractions were the primary P forms in sediments of Lake Burgäschi (Fig. 6 and 8). This
425 seems to compare well with the study of Moosmann et al. (2006), who suggested that sediment Fe contents control
426 P retention in sediments of the Swiss Plateau lakes. However, after ~1977, we observed a change to predominantly
427 Ca-P (apatite-P), occurring concurrently with the operation of hypolimnetic withdrawal restoration. This clear
428 pattern in sedimentary P-fraction change can be largely attributed to this restoration measure. The hypolimnetic
429 withdrawal treatment in Lake Burgäschi removes not only hypolimnetic P but also dissolved metal (Al, Fe and
430 Mn) ions and, thus leads to calcite as the main sorbent for P in upper waters and to an enhanced proportion of Ca-
431 P fraction in sediments.

432

433 In spite of the effects of lake restoration on sedimentary P retention in Zone IV, overall, the retention of total P
434 and labile P fractions in the sediment profile was mainly controlled by autochthonous Fe (Fe/Ti), Mn, and
435 hypolimnetic oxygenation proxy-Fe/Mn ratios, as shown by the results of RDA analysis (Fig. 7). Our results
436 support the previous suggestion that long-term permanent sediment-P retention is largely limited by the sediment's
437 binding capacity in anoxic conditions (Moosmann et al., 2006; Hupfer and Lewandowski, 2008), which,
438 specifically in our case, is determined by redox-sensitive elements (autochthonous Fe and Mn) preserved in
439 sediments. These findings are discussed in the context of each cluster zone as follows: During Zone I and Zone
440 III, when the hypolimnion had better seasonally oxic conditions (see Fig. 8 and Fig. S11), the increased retention
441 of Mn and Fe, and labile P fractions occurred simultaneously (Fig. 3 and 5). This phenomenon might be caused
442 by efficient P-trapping in Mn- and Fe enriched layers. It has been suggested that the formation of laminated Mn-
443 and Fe enriched layers could serve as a protective cap to reduce P release from surface sediment layers to the
444 anoxic hypolimnion (Żarczyński et al., 2018) which, thus, can help improve P retention within these sedimentary
445 layers. In Zone II, small amounts of labile P fractions might result from decreased P-bearing solid phases (Mn and
446 Fe minerals) in sediments under anoxic conditions in the hypolimnion (see higher Fe/Mn ratios in Sect. 5.2; Fig.
447 S11). However, in Zone IV, we observed the lowest retention and NBR of total P and labile P fractions in recent
448 sediments (Fig. 5; Fig. S9). We interpret this as a combined result of eutrophication-induced hypolimnetic anoxia
449 and hypolimnetic withdrawal since 1977 whereby P-rich hypolimnetic water is discharged out of the lake. On the
450 one hand, under stable anoxic conditions in the hypolimnion caused by strong eutrophication, reduced Mn and Fe
451 preservation (Fig. 3) suggests a low capacity of permanent P-trapping within the anoxic sediments. On the other

455 hand, hypolimnetic withdrawal restoration in Lake Burgäschi has substantially reduced hypolimnetic P
456 concentrations by a factor of 5-6 since 1978 (Fig. S11; GSA, 2007) and MARs (Fig. 2c and Fig. S9). This indicates
457 a concomitant decrease in sediment-P release to the hypolimnion and P sedimentation to the water-sediment
458 interface (gross sedimentation of P) as well. Consequently, decreased total P concentrations and total P-NBR in
459 sediments were observed (Fig. 6a and S9). The reduction of total P contents in upper sediments caused by
460 hypolimnetic withdrawal was also reported from Lake Kortowskie of Poland (Dunalska et al., 2007). Moreover,
461 our findings confirm that this restoration is an effective method to reduce sediment-P release potentials, as
462 indicated by considerably decreased NBR of labile P fractions in upper sediments (Fig. S9).

463

464 In the whole sediment profile, HCl-P and Ref.-P_o fractions had mainly autochthonous origins and were mainly
465 controlled by in-lake processes rather than by clastic inputs (e.g. apart from molasses sandstone), as indicated by
466 absent positive correlations between the two fractions and detrital elements such as Ti, K and Al (Fig. 7). HCl-P
467 (i.e. Ca-P) fraction retention, to a large extent, resulted from authigenic CaCO₃-P precipitation, and increased with
468 higher eutrophic levels in Zone III and IV (Fig. 5; Sect. 5.1). We interpret this as an incidence of biologically
469 driven co-precipitation of Ca and P in highly productive lakes. The phenomenon of Ca-P co-precipitation has been
470 observed and studied in many calcareous lakes (Dittrich and Koschel 2002; Whitehouse, 2010), and is assumed to
471 be responsible for the scavenging of dissolved P from surface waters of eutrophic lakes (Hamilton et al., 2009). In
472 addition, large amounts of Ca-P in surface sediments (top 21 cm) can act as a potential negative feedback to
473 eutrophication in Lake Burgäschi, because Ca-P fraction is relatively stable in sediments and has low potentials of
474 P-release from surface sediments back to lake waters. Interestingly, HCl-P fraction retention and NBR in sediments
475 of Zone IV were generally lower than in Zone III (Fig. 5 and Fig. S9), although the lake in Zone IV had relatively
476 higher eutrophic levels (see Sect. 5.1; Fig. S11). The pH in the hypolimnion of Lake Burgäschi varied between 7.0
477 and 7.5 according to the monitoring data in 1993, 2003, and 2013 (Guthruf et al., 2013). Therefore, the acid
478 dissolution of Ca-P in the hypolimnion and at the water-sediment interface is small and unlikely significant during
479 Zone IV. The generally decreased retention and NBR of Ca-P fraction were seemingly related to hypolimnetic
480 withdrawal, which has caused lower water-P concentrations and MAR of sediments as discussed above. As a result,
481 there are reductions of CaCO₃-P co-precipitation in the epilimnion and consequently of Ca-P net sedimentation in
482 surface sediments. Overall, Ref.-P_o fraction retention and NBR in the sedimentary profile show less variability
483 compared with other P fractions (Fig. 5 and Fig. S9). Nevertheless, the lower NBR of Ref.-P_o fraction in the upper
484 sediments (~ top 10 cm) could be derived from the ongoing early degradation of fresh organic matters.

485

486 The interesting observation is that the water-P reductions caused by the hypolimnetic withdrawal in Lake
487 Burgäschi (GSA, 2007; Nürnberg, 2007) have been ineffective in reducing algal blooms and curbing
488 eutrophication. Similar findings were also reported from some lakes in Europe and the US (Kosten et al., 2012;
489 Kolzau et al., 2014; Fastner et al., 2016). These authors have attributed this phenomenon to insufficient external
490 P-load reduction, higher water temperatures under global warming of the last few decades, and the light or nitrogen
491 limitation of surface-water phytoplankton. In Lake Burgäschi, phytoplankton growth in the trophic zone is more
492 likely limited by P during growth season after 1978 rather than by the nitrogen (GSA, 2007) as the algae-available
493 ortho-phosphate is almost completely used up in the epilimnion when the nitrate concentrations stay as high as
494 0.5-3 mg N / L in the upper 5-m waters (GBL, 1995). Hence, we suggest that these factors mentioned above,

Deleted: still

Deleted: mostly

497 except for nitrogen limitation of lake productivity, may also contribute to promoting persistently high primary
498 productivity in Lake Burgäschi. But the main driver keeping productivity high, is the continuing high external P
499 loads from the lake catchment. During summer stratification, ~~the high lake external P load~~ into the epilimnion
500 primarily supports phytoplankton growth in the photic zone, which is not strongly influenced by the hypolimnetic-
501 P discharge and internal P loadings. From a management perspective, it is still critically important to focus on
502 lowering external P loads in order to decrease primary production and eutrophication in seasonally-stratified small
503 deep lakes which are more likely to favor stable stratification during phytoplankton growth season.

504

505 **6 Conclusion**

506 This study shows that in Lake Burgäschi, more than half of sediment P is buried in relatively labile P fractions
507 (Fe/Mn/Al-P), yet with low potentials for P-release from these labile P fractions in deeper layers (below ~21 cm).
508 Our results highlight the importance of hypolimnetic oxygenation/mixing regime in controlling long-term P
509 retention and net burial rates of labile P fractions in sediments of this small deep lake. Irrespective of increasing
510 lake primary productivity during early 1900s to 1977, the two periods of high sedimentary retention of total P and
511 labile P-fraction occurred in Fe- and Mn enriched laminae, which appears to be linked to seasonal mixing of the
512 hypolimnion in the past. Importantly, the positive effects of hypolimnetic withdrawal in Lake Burgäschi were
513 observed primarily in sediment P-fraction data but not in lake trophic state. The 40-year operation of hypolimnetic
514 withdrawal has impoverished sedimentary P, in particular largely decreased net burial rates of labile P fractions
515 (potential internal P loads), and increased the relative proportion of stable Ca-P fraction in top sediment layers (0-
516 21 cm). Nevertheless, the lake is currently still highly eutrophic. We attribute the delay of lake recovery primarily
517 to still high nutrient inputs from the nearby or surrounding agricultural area into the lake trophic zone during
518 stratification seasons. This study calls for consistently more effective measures to minimize external P loadings
519 from the catchment, such as optimizing fertilizer application practices and technical measures in the drainages.

520

521

522

523 **Data availability**

524 The data is available at PANGAEA at <https://doi.pangaea.de/10.1594/PANGAEA.908896>.

525

526

527 **Author contributions**

528 L.T. helped with sample collection, analyzed the sediment, conducted data analysis, wrote the manuscript, and
529 acquired most of the funding for the project.

530 P. Z. helped with sediment core subsampling, conducted the hyperspectral imaging (HSI) scanning, helped with
531 XRF-scanning, substantially contributed to the data interpretation.

532 S.S. measured gamma-spectroscopy radiometric activities, generated the data for chronology and helped with
533 data interpretation.

534 R.L. conducted the XRF-scanning and helped with data interpretation.

535 M.G. designed the study, helped discussing the results, editing the manuscript and supervised the project.

536 All authors commented on the manuscript.

Deleted: the

Deleted: high loads of P

Deleted: lake

Deleted: will be made

541

542 **Competing interests**

543 The authors declare that they have no conflict of interest.

544

545 **Acknowledgements**

546 We thank Stamatina Makri and Dr. Andre F. Lotter for their help during the fieldwork. We thank Irene Brunner,
547 Patrick Neuhaus, Dr. Daniela Fischer and Andrea Sanchini for their expertise and the lab assistance. Further, we
548 acknowledge Dr. Klaus A. Jarosch for the valuable suggestions about phosphorus data. The thoughtful comments
549 and suggestion by the two anonymous reviewers greatly improved this paper. The project was funded by the Swiss
550 National Science Foundation under the grant number 200021-172586, a Fellowship Grant from the Chinese
551 Scholarship Counsel and the International PhD Fellowship from University of Bern.

552

553

554 **References**

- 555 Anthony, R. S.: Iron-rich rhythmically laminated sediments in Lake of the Clouds, northeastern Minnesota, *Limnol.*
556 *Oceanogr.*, 22, 45–54, <https://doi.org/10.4319/lo.1977.22.1.0045>, 1977.
- 557 Appleby, P.G.: Chronostratigraphic techniques in recent sediments, In: *Tracking Environmental Change Using*
558 *Lake Sediments. Basin Analysis, Coring, and Chronological Techniques*, edited by: Last, W.M., and Smol, J.P.,
559 Springer, Dordrecht, Netherlands, 171-203, https://doi.org/10.1007/0-306-47669-X_9, 2002.
- 560 Bennett, K. D.: Determination of the number of zones in a biostratigraphical sequence, *New Phytol.*, 132, 155–
561 170, <https://doi.org/10.1111/j.1469-8137.1996.tb04521.x>, 1996.
- 562 Binderheim-Bankay, E. A.: *Sanierungsziel für natürlich eutrophe Kleinseen des Schweizer Mittellandes*, Ph.D.
563 thesis, ETH Zurich, Switzerland, 149 pp., 1998.
- 564 Bonk, A., Kinder, M., Enters, D., Grosjean, M., Meyer-Jacob, C., and Tylmann, W.: Sedimentological and
565 geochemical responses of Lake Żabińskie (north-eastern Poland) to erosion changes during the last millennium, *J.*
566 *Paleolimnol.*, 56, 239–252, <https://doi.org/10.1007/s10933-016-9910-6>, 2016.
- 567 Boyle, J. F.: Inorganic Geochemical Methods in Palaeolimnology, In: *Tracking Environmental Change Using Lake*
568 *Sediments. Basin Analysis, Coring, and Chronological Techniques*, edited by: Last, W.M., and Smol, J.P., Springer,
569 Dordrecht, Netherlands, 83-141, https://doi.org/10.1007/0-306-47670-3_5, 2002.
- 570 Büren, G. von: *Der Burgäschisee*, Mitteilungen der Naturforschenden Gesellschaft, Bern, 83 pp., 1949.
- 571 Burley, K.L., Prepas, E.E., and Chambers, P.A.: Phosphorus release from sediments in hardwater eutrophic lakes:
572 the effects of redox-sensitive and-insensitive chemical treatments, *Freshwater Biol.*, 46, 1061–1074,
573 <https://doi.org/10.1046/j.1365-2427.2001.00789.x>, 2001.
- 574 Butz, C., Grosjean, M., Fischer, D., Wunderle, S., Tylmann, W., and Rein, B.: Hyperspectral imaging spectroscopy:
575 a promising method for the biogeochemical analysis of lake sediments, *J. Appl. Remote Sens.*, 9, 1–20,
576 <https://doi.org/10.1117/1.JRS.9.096031>, 2015.
- 577 Butz, C., Grosjean, M., Goslar, T., and Tylmann, W.: Hyperspectral imaging of sedimentary bacterial pigments: a
578 1700-year history of meromixis from varved Lake Jaczno, northeast Poland, *J. Paleolimnol.*, 58, 57–72,

579 <https://doi.org/10.1007/s10933-017-9955-1>, 2017.

580 Cavalcante, H., Araujo, F. Noyma, N.P., and Becker, V.: Phosphorus fractionation in sediments of tropical
581 semiarid reservoirs. *Sci. Total Environ.*, 619-620, 1022–1029, <https://doi.org/10.1016/j.scitotenv.2017.11.204>,
582 2018

583 Chen, M., Ding, S., Chen, X., Sun, Q., Fan, X., Lin, J., Ren, M., Yang, L., and Zhang, C.: Mechanisms driving
584 phosphorus release during algal blooms based on hourly changes in iron and phosphorus concentrations in
585 sediments, *Water res.*, 133, 153–164. <https://doi.org/10.1016/j.watres.2018.01.040>, 2018.

586 Dittrich, M. and Koschel, R.: Interactions between calcite precipitation (natural and artificial) and phosphorus
587 cycle in the hardwater lake, *Hydrobiologia*, 469, 49–57, <https://doi.org/10.1023/A:1015571410442>, 2002.

588 Dunalska, J.A., Wiśniewski, G., and Mientki, C.: Assessment of multi-year (1956-2003) hypolimnetic withdrawal
589 from Lake Kortowskie, Poland, *Lake and Reserv. Manage.*, 23, 377-387,
590 <https://doi.org/10.1080/07438140709354025>, 2007.

591 Einsele, W.: Über die Beziehungen des Eisenkreislaufs zum Phosphatkreislauf im eutrophen See, *Arch. Hydrobiol.*,
592 29, 664–686, 1936.

593 Einsele, W.: Über chemische und kolloidchemische Vorgänge in Eisen-Phosphat- Systemen unter limnischen and
594 limnogeologischen Gesichtspunkten, *Arch. Hydrobiol.*, 33, 361–387, 1938.

595 Enters, D., Lücke, A., and Zolitschka, B.: Effects of land-use change on deposition and composition of organic
596 matter in Frickenhauser See, northern Bavaria, Germany, *Sci. Total Environ.*, 369, 178–187,
597 <https://doi.org/10.1016/j.scitotenv.2006.05.020>, 2006.

598 Fastner, J., Abella, S., Litt, A., Morabito, G., Vörös, L., Pálffy, K., Straile, D., Kümmerlin, R., Matthews, D.,
599 Phillips, M.G., and Chorus, I.: Combating cyanobacterial proliferation by avoiding or treating inflows with high
600 P load—experiences from eight case studies, *Aquat. Ecol.*, 50, 367–383, <https://doi.org/10.1007/s10452-015-9558-8>, 2016.

601

602 Frugone-Álvarez, M., Latorre, C., Giralt, S., Polanco-Martínez, J., Bernárdez, P., Oliva-Urcia, B., Maldonado, A.,
603 Carrevedo, M.L., Moreno, A., Delgado Huertas, A., and Prego, R.: A 7000-year high-resolution lake sediment
604 record from coastal central Chile (Lago Vichuquén, 34° S): implications for past sea level and environmental
605 variability, *J. Quaternary Sci.*, 32, 830–844, <https://doi.org/10.1002/jqs.2936>, 2017.

606 Gächter, R.: Die Tiefenwasserableitung, ein Weg zur Sanierung von Seen, *Schweizerische Zeitschrift für*
607 *Hydrologie*, 38, 1–28, 1976.

608 Gächter, R.: Lake restoration. Why oxygenation and artificial mixing cannot substitute for a decrease in the
609 external phosphorus loading, *Aquat. Sci.*, 49, 176–185, <https://doi.org/10.1007/BF02538501>, 1987.

610 Gächter, R. and Wehrli, B.: Ten years of artificial mixing and oxygenation: no effect on the internal phosphorus
611 loading of two eutrophic lakes, *Environ. Sci. Technol.*, 32, 3659–3665, <https://doi.org/10.1021/es980418>, 1998.

612 Gächter, R. and Müller, B.: Why the phosphorus retention of lakes does not necessarily depend on the oxygen
613 supply to their sediment surface, *Limnol. Oceanogr.*, 48, 929–933, <https://doi.org/10.4319/lo.2003.48.2.0929>,
614 2003.

615 Giguet-Covex, C., Arnaud, F., Poulernard, J., Enters, D., Reyss, J.L., Millet, L., Lazzaroto, J., and Vidal, O.:
616 Sedimentological and geochemical records of past trophic state and hypolimnetic anoxia in large, hard-water Lake
617 Bourget, French Alps, *J. Paleolimnol.*, 43, 171–190, <https://doi.org/10.1007/s10933-009-9324-9>, 2010.

618 Gonsiorczyk, T., Casper, P., and Koschel, R.: Phosphorus-binding forms in the sediment of an oligotrophic and an
619 eutrophic hardwater lake of the Baltic Lake District (Germany), *Water Sci. Technol.*, 37, 51–58,
620 [https://doi.org/10.1016/S0273-1223\(98\)00055-9](https://doi.org/10.1016/S0273-1223(98)00055-9), 1998.

621 Grimm, E. C.: CONISS: a FORTRAN 77 program for stratigraphically constrained cluster analysis by the method
622 of incremental sum of squares, *Comput. Geosci.*, 13, 13–35, [https://doi.org/10.1016/0098-3004\(87\)90022-7](https://doi.org/10.1016/0098-3004(87)90022-7), 1987.

623 Guthruf, J., Zeh, M., and Guthruf-Seiler, K.: Kleinseen im Kanton Bern, Water Protection and Waste Management
624 Office of the Canton of Bern, Bern, 1999.

625 Guthruf, K., Maurer, V., Ryser, R., Zeh, M., and Zweifel, N.: Zustand der Kleinseen, Construction, Transport and
626 Energy Directorate of the Canton of Bern Office for Water and Waste Water and soil protection laboratory, Bern,
627 2013.

628 Håkanson, L. and Jansson, M. (Eds.): *Principles of Lake Sedimentology*, The Blackburn Press, New Jersey, USA,
629 2002.

630 Hamilton, S.K., Bruesewitz, D.A., Horst, G.P., Weed, D.B., and Sarnelle, O.: Biogenic calcite–phosphorus
631 precipitation as a negative feedback to lake eutrophication, *Can. J. Fish. Aquat. Sci.*, 66, 343–
632 350, <https://doi.org/10.1139/F09-003>, 2009.

633 Heiri, O., Lotter, A. F., and Lemcke, G.: Loss on ignition as a method for estimating organic and carbonate content
634 in sediments: reproducibility and comparability of results, *J. Paleolimnol.*, 25, 101–110,
635 <https://doi.org/10.1023/A:1008119611481>, 2001.

636 Holmer, M. and Storkholm, P.: Sulphate reduction and sulphur cycling in lake sediments: a review, *Freshwater
637 Biol.*, 46, 431–451, <https://doi.org/10.1046/j.1365-2427.2001.00687.x>, 2001.

638 Hupfer, M. and Lewandowski, J.: Oxygen controls the phosphorus release from lake sediments—a long-lasting
639 paradigm in limnology, *Int. Rev. Hydrobiol.*, 93, 415–432, <https://doi.org/10.1002/iroh.200711054>, 2008.

640 Juggins, S.: rioja: analysis of quaternary science data, <https://cran.r-project.org/web/packages/rioja/index.html>,
641 2017.

642 Kaiserli, A., Voutsas, D., and Samara, C.: Phosphorus fractionation in lake sediments—lakes Volvi and Koronia,
643 N. Greece, *Chemosphere*, 46, 1147–1155, [https://doi.org/10.1016/S0045-6535\(01\)00242-9](https://doi.org/10.1016/S0045-6535(01)00242-9), 2002.

644 Kolzau, S., Wiedner, C., Rucker, J., Köhler, J., Köhler, A., and Dolman, A. M.: Seasonal patterns of nitrogen and
645 phosphorus limitation in four German lakes and the predictability of limitation status from ambient nutrient
646 concentrations, *Plos One*, 9, e96065, <https://doi.org/10.1371/journal.pone.0096065>, 2014.

647 Kosten, S., Huszar, V.L., Bécares, E., Costa, L.S., van Donk, E., Hansson, L.A., Jeppesen, E., Kruk, C., Lacerot,
648 G., Mazzeo, N., and De Meester, L.: Warmer climates boost cyanobacterial dominance in shallow lakes, *Global
649 Change Biol.*, 18, 118–126, <https://doi.org/10.1111/j.1365-2486.2011.02488.x>, 2012.

650 Kucklentz, V. and Hamm, A. (Eds.): *Möglichkeiten und Erfolgsaussichten der Seenrestaurierung*, Bayrische
651 Landesanstalt für Wasserforschung, München, Germany, 212 pp., 1988.

652 LAWA (Länderarbeitsgemeinschaft Wasser): *Gewässerbewertung — stehende Gewässer: Richtlinie für die
653 Bewertung nach trophischen Kriterien*, Germany, 1998.

654 Lukkari, K., Hartikainen, H., and Leivuori, M.: Fractionation of sediment phosphorus revisited. I: Fractionation
655 steps and their biogeochemical basis, *Limnol. Oceanog- Meth.*, 5, 433–444,
656 <https://doi.org/10.4319/lom.2007.5.433>, 2007.

657 Mackereth, F.J.H.: Some chemical observations on post-glacial lake sediments, *Philos. T. Roy. Soc. B.*, 250, 165–
658 213, <https://doi.org/10.1098/rstb.1966.0001>, 1966.

659 GBL. Burgäschisee. Resultate der Wasser- und Planktonuntersuchungen 1977-1995. Office for Water Protection
660 and Waste Management of the Canton of Bern, 1995.

661 GSA: 30 Jahre Tiefenwasser-Ableitung. Wie geht es dem Burgäschisee heute?, Office for Water Protection and
662 Waste Management of the Canton of Bern, Bern, 2007.

663 McCulloch, J., Gudimov, A. Arhonditsis, G. Chesnyuk, A., and Dittrich, M.: Dynamics of P-binding forms in
664 sediments of a mesotrophic hard-water lake: Insights from non-steady state reactive-transport modeling, sensitivity
665 and identifiability analysis, *Chem. Geol.*, 354, 216–232, <https://doi.org/10.1016/j.chemgeo.2013.06.011>, 2013.

666 Meyers, P. A. and Ishiwatari, R.: Lacustrine organic geochemistry—an overview of indicators of organic matter
667 sources and diagenesis in lake sediments, *Org. Geochem.*, 20, 867–900, [http://dx.doi.org/10.1016/0146-](http://dx.doi.org/10.1016/0146-6380(93)90100-P)
668 [6380\(93\)90100-P](http://dx.doi.org/10.1016/0146-6380(93)90100-P), 1993,

669 Michel, H., Barci-Funel, G., Dalmasso, J., Ardisson, G., Appleby, P., Haworth, E., and El-Daouhy, F.: Plutonium,
670 americium and cesium records in sediment cores from Blelham Tarn, Cumbria (UK), *J. Radioanal. Nucl. Ch.*, 247,
671 107–110, <https://doi.org/10.1023/A:1006719215833>, 2001.

672 Moosmann, L., Gächter, R. Müller, B., and Wüest, A.: Is phosphorus retention in autochthonous lake sediments
673 controlled by oxygen or phosphorus?, *Limnol. Oceanogr.*, 51, 763–771,
674 https://doi.org/10.4319/lo.2006.51.1_part_2.0763, 2006.

675 Mikomägi, A., Koff, T., Martma, T., and Marzecová, A.: Biological and geochemical records of human-induced
676 eutrophication in a small hard-water lake, *Boreal Env. Res.*, 21, 513–527, 2016.

677 Naeher, S., Gilli, A., North, R.P., Hamann, Y., and Schubert, C.J.: Tracing bottom water oxygenation with
678 sedimentary Mn/Fe ratios in Lake Zurich, Switzerland, *Chem. Geol.*, 352, 125–133,
679 <https://doi.org/10.1016/j.chemgeo.2013.06.006>, 2013.

680 Nikolai, S.J. and Dzialowski, A.R.: Effects of internal phosphorus loading on nutrient limitation in a eutrophic
681 reservoir, *Limnologica*, 49, 33–41, <https://doi.org/10.1016/j.limno.2014.08.005>, 2014.

682 Nürnberg, G.K.: Lake responses to long-term hypolimnetic withdrawal treatments, *Lake Reserv. Manage.*, 23,
683 388–409, <https://doi.org/10.1080/07438140709354026>, 2007.

684 Ogdahl, M. E., Steinman, A. D., and Weinert, M. E.: Laboratory-determined phosphorus flux from lake sediments
685 as a measure of internal phosphorus loading, *Jove-J. Vis. Exp.*, 85, e51617, <https://dx.doi.org/10.3791%2F51617>,
686 2014.

687 Oksanen, J., Blanchet, F.G., Kindt, R., Legendre, P., Minchin, P.R., O'hara, R., Simpson, G.L., Solymos, P.,
688 Stevens, M.H.H., and Wagner, H.: Package 'vegan'. Community ecology package, version 2, [http://cran.r-](http://cran.r-project.org/web/packages/vegan/index.html)
689 [project.org/web/packages/vegan/index.html](http://cran.r-project.org/web/packages/vegan/index.html), 2013.

690 Pennington, W., Tutin, T.G., Cambray, R.S., and Fisher, E.M.: Observations on lake sediments using fallout ¹³⁷Cs
691 as a tracer, *Nature*, 242, 324–326, <https://doi.org/10.1038/242324a0>, 1973.

692 R Development Core Team: R: A Language and Environment for Statistical Computing, R Foundation for
693 Statistical Computing, Vienna, Austria, 2017.

694 Rentz, J., Turner, I.P., and Ullman, J.L.: Removal of phosphorus from solution using biogenic iron oxides, *Water*
695 *Res.*, 43, 20292035, <https://doi.org/10.1016/j.watres.2009.02.021>, 2009.

696 Reuss, N., Conley, D.J., and Bianchi, T.S.: Preservation conditions and the use of sediment pigments as a tool for
697 recent ecological reconstruction in four Northern European estuaries, *Mar. Chem.*, 95, 283–302,
698 <https://doi.org/10.1016/j.marchem.2004.10.002>, 2005.

699 Rey, F., Gobet, E., van Leeuwen, J.F.N., Gilli, A., van Raden, U.J., Hafner, A., Wey, O., Rhiner, J., Schmockler,
700 D., Zünd, J., and Tinner, W.: Vegetational and agricultural dynamics at Burgäschisee (Swiss Plateau) recorded for
701 18,700 years by multi-proxy evidence from partly varved sediments, *Veg. Hist. Archaeobot.*, 26, 571–586.
702 <https://doi.org/10.1007/s00334-017-0635-x>, 2017.

703 Ribeiro, D., Martins, G., Nogueira, R., Cruz, J.V., and Brito, A.: Phosphorus fractionation in volcanic lake
704 sediments (Azores–Portugal), *Chemosphere*, 70, 1256–1263, <https://doi.org/10.1016/j.chemosphere.2007.07.064>,
705 2008.

706 Richter, T.O., Van der Gaast, S., Koster, B., Vaars, A., Gieles, R., de Stigter, H.C., De Haas, H., and van Weering,
707 T.C.: The Avaatech XRF Core Scanner: technical description and applications to NE Atlantic sediments, *Geol.*
708 *Soc. London Spec. Publ.*, 267, 39–50, <https://doi.org/10.1144/GSL.SP.2006.267.01.03>, 2006.

709 Rydin, E.: Potentially mobile phosphorus in Lake Erken sediment. *Water Res.*, 34, 2037–2042,
710 [https://doi.org/10.1016/S0043-1354\(99\)00375-9](https://doi.org/10.1016/S0043-1354(99)00375-9), 2000.

711 Schmid, S.M., Fügenschuh, B., Kissling, E., and Schuster, R.: Tectonic map and overall architecture of the
712 Alpine orogen, *Eclogae Geol. Helv.*, 97, 93–117, <https://doi.org/10.1007/s00015-004-1113-x>, 2004.

713 Schneider, T., Rimer, D., Butz, C., and Grosjean, M.: A high-resolution pigment and productivity record from
714 the varved Ponte Tresa basin (Lake Lugano, Switzerland) since 1919: insight from an approach that combines
715 hyperspectral imaging and highperformance liquid chromatography, *J. Paleolimnol.*, 60, 381–398,
716 <https://doi.org/10.1007/s10933-018-0028-x>, 2018.

717 Schnurrenberger, D., Russell, J., and Kelts, K.: Classification of lacustrine sediments based on sedimentary
718 components, *J. Paleolimnol.*, 29, 141–154, <https://doi.org/10.1023/A:1023270324800>, 2003.

719 Smith, L., Watzin, M. C., and Druschel, G.: Relating sediment phosphorus mobility to seasonal and diel redox
720 fluctuations at the sediment-water interface in a eutrophic freshwater lake, *Limnol. and Oceanogr.*, 56, 2251–
721 2264, <https://doi.org/10.4319/lo.2011.56.6.2251>, 2011.

722 Søndergaard, M., Jensen, P.J., and Jeppesen, E.: Retention and internal loading of phosphorus in shallow,
723 eutrophic lakes, *Sci. World J.*, 1, 427–442, <https://doi.org/10.1100/tsw.2001.72>, 2001

724 Stevens, L., Ito, E., and Olson, D.: Relationship of Mn-carbonates in varved lake-sediments to catchment
725 vegetation in Big Watab Lake, MN, USA. *J. Paleolimnol.*, 24, 199–211,
726 <https://doi.org/10.1023/A:1008169526577>, 2000.

727 Trolle, D., Hamilton, D.P., and Pilditch, C.A.: Evaluating the influence of lakemorphology, trophic status and
728 diagenesis on geochemical profiles in lake sediments, *Appl. Geochem.*, 25, 621–632,
729 <https://doi.org/10.1016/j.apgeochem.2010.01.003>, 2010.

730 Tu, L., Jarosch, K.A., Schneider, T., and Grosjean, M.: Phosphorus fractions in sediments and their relevance for
731 historical lake eutrophication in the Ponte Tresa basin (Lake Lugano, Switzerland) since 1959, *Sci. Total Environ.*,
732 685, 806–817, <https://doi.org/10.1016/j.scitotenv.2019.06.243>, 2019.

733 Tylmann, W., Bonk, A., Goslar, T., Wulf, S., and Grosjean, M.: Calibrating ²¹⁰Pb dating results with varve
734 chronology and independent chronostratigraphic markers: Problems and implications, *Quat. Geochronol.* 32, 1–
735 10, <https://doi.org/10.1016/j.quageo.2015.11.004>, 2016.

736 van Raden, U. J.: High-resolution Swiss lake records of climate change. Ph.D. thesis, ETH Zurich, Switzerland,
737 <https://doi.org/10.3929/ethz-a-009783578>, 2012.

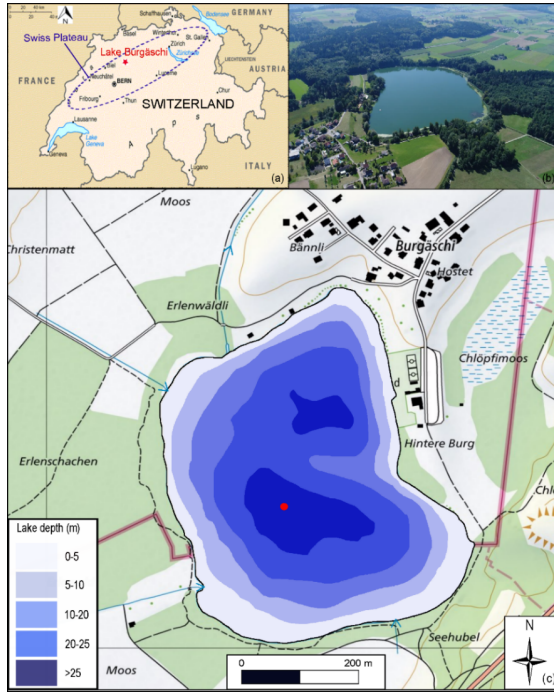
738 Whitehouse, R.D.: Phosphorus scavenging through calcite co-precipitation: bringing clarity to Clear Lake, B.Sc.
739 thesis, University of British Columbia, Canada, 2010.

740 Wirth, S.B., Gilli, A., Niemann, H., Dahl, T.W., Ravasi, D., Sax, N., Hamann, Y., Peduzzi, R., Peduzzi, S., Tonolla,
741 M., and Lehmann, M.F.: Combining sedimentological, trace metal (Mn, Mo) and molecular evidence for
742 reconstructing past water-column redox conditions: The example of meromictic Lake Cadagno (Swiss Alps),
743 *Geochim. Cosmochim. Ac.*, 120, 220–238, <https://doi.org/10.1016/j.gca.2013.06.017>, 2013.

744 Żarczyński, M., Wacnik, A., and Tylmann, W.: Tracing lake mixing and oxygenation regime using the Fe/Mn
745 ratio in varved sediments: 2000year-long record of human-induced changes from Lake Zabinskie (NE Poland),
746 *Sci. Total Environ.*, 657, 585–596, <https://doi.org/10.1016/j.scitotenv.2018.12.078>, 2019.

747 Żarczyński, M., Tylmann, W., and Goslar, T.: Multiple varve chronologies for the last 2000 years from the
748 sediments of Lake Żabińskie (northeastern Poland)–Comparison of strategies for varve counting and uncertainty
749 estimations, *Quaternary Geochronology*, 47, 107–119, <https://doi.org/10.1016/j.quageo.2018.06.001>, 2018.

750
751
752
753
754
755
756
757
758
759
760
761
762
763
764



765

766 **Figure 1: Study site. (a) Overview map of Switzerland and the Swiss Plateau. Lake Burgäschi is indicated as the**
 767 **asterisk. (b) Photo of Lake Burgäschi and catchment (© 2018 Google Maps). (c) Bathymetric map of Lake Burgäschi**
 768 **adapted from Guthruf et al. (1999). The red dot indicates the coring site (color figure online). Green areas around the**
 769 **lake indicate forests, white areas agricultural lands. Inflow and outflow to the lake are indicated by blue arrow lines**
 770 **(topographic maps: © swisstopo).**

771

772

773

774

775

776

777

778

779

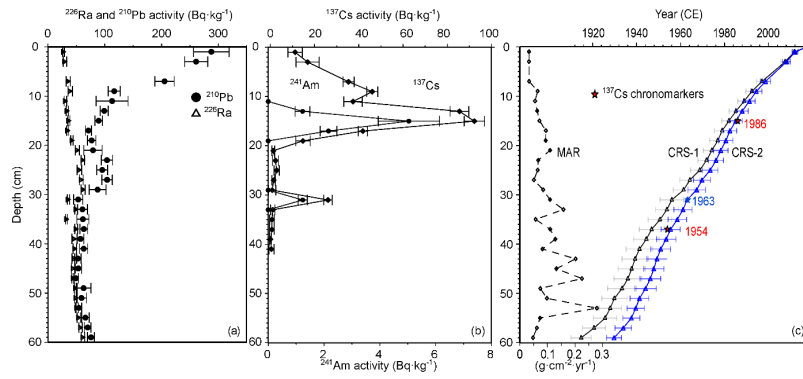
780

781

782

783

784



785

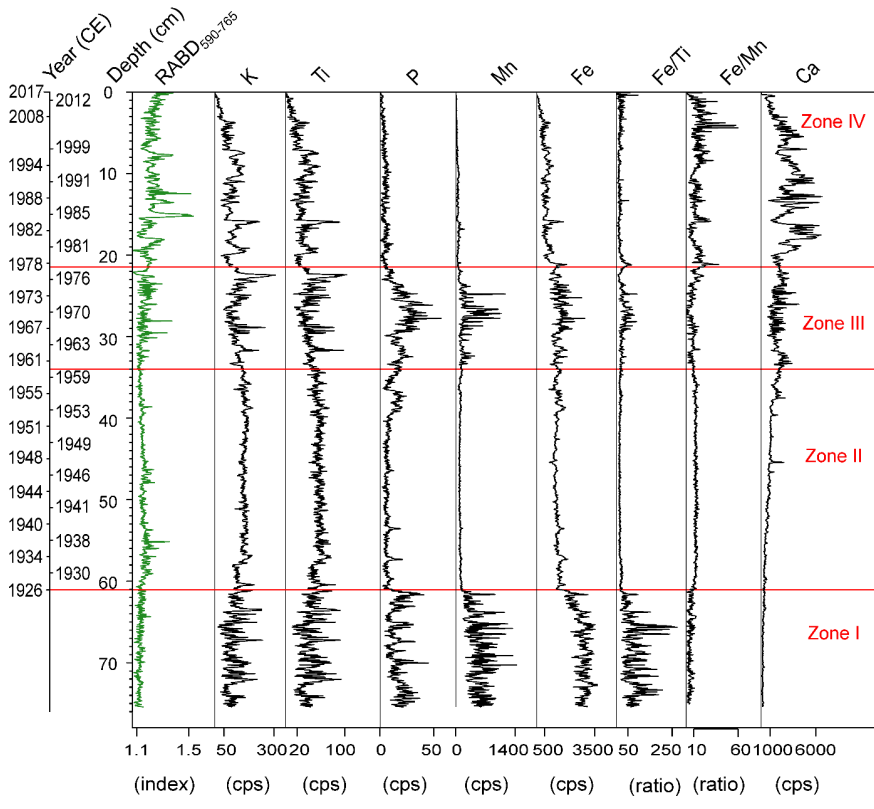
786 **Figure 2: (a) Total ^{210}Pb , ^{226}Ra , and (b) ^{137}Cs and ^{241}Am activity concentration profiles in sediment core Burg17-B from**
787 **Lake Burgäschi; (c) The comparison of different ^{210}Pb CRS models: unconstrained CRS-1 model and constrained CRS-**
788 **2 model at 1963; the mass accumulation rates (MAR) are obtained from the CRS-2 model.**

789

790

791

792

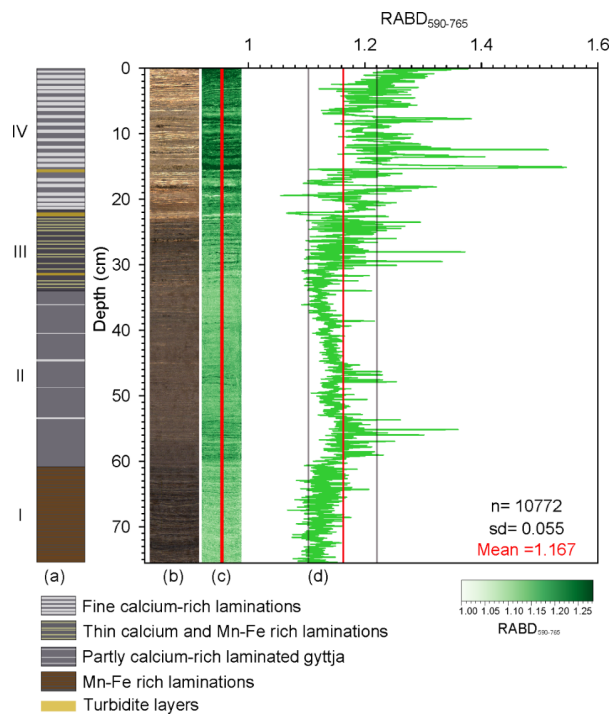


793

794 **Figure 3: Stratigraphic records of HSI-inferred green-pigments (RABD₅₉₀₋₇₆₅) and XRF-data in sediments of core**
 795 **Burg17-B. Elemental counts are represented in cps (counts per second). The red horizontal lines separate the four**
 796 **significant clusters retrieved by the CONISS analysis (color figure online).**

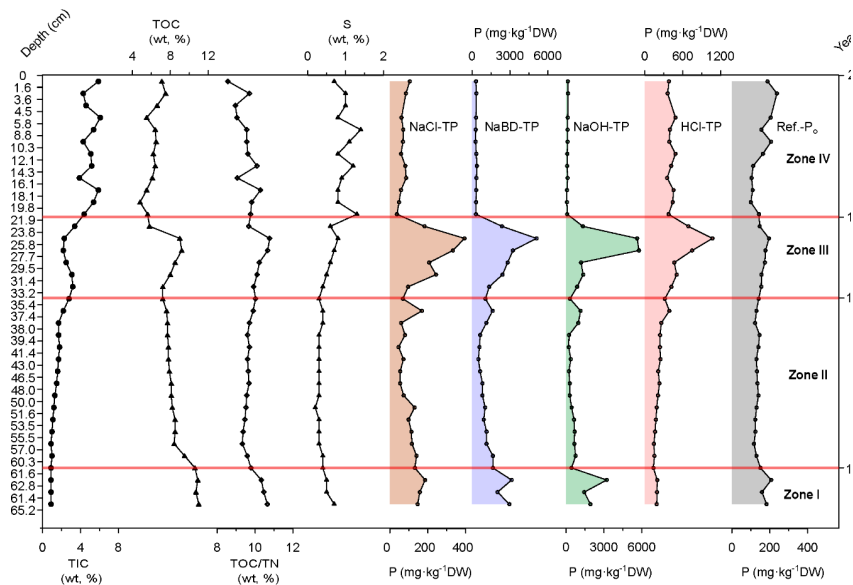
797

798



799

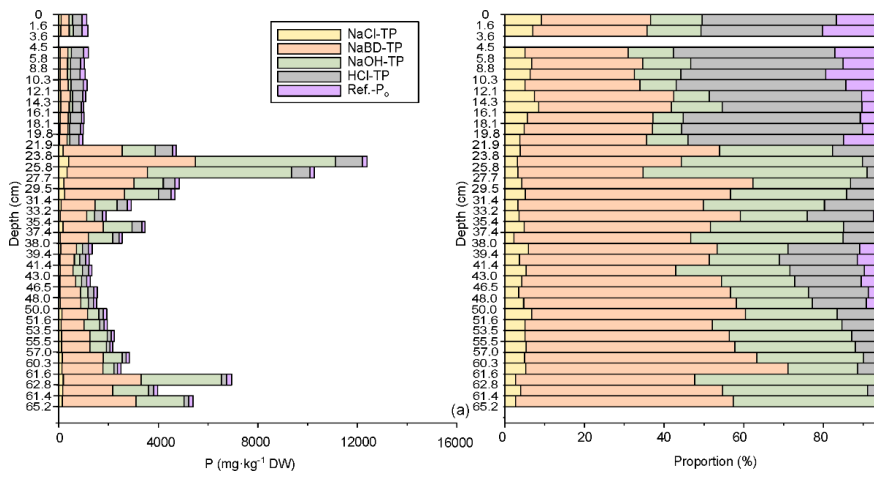
800 Figure 4: (a) Lithological description of Burg17-B sediment core. The intensities of Ca, Fe and Mn in each unit were
 801 inferred from XRF-element counts in Fig. 3; Yellow colors highlight the turbidite layers identified from the XRF peaks
 802 of siliciclastic elements e.g. K, Ti, and Rb. (b) RGB contrast enhanced sediment core picture. (c) The map of the spectral
 803 index RABD₅₉₀₋₇₆₅ (i.e. green-pigments) distribution, and (d) the graphic output of RABD₅₉₀₋₇₆₅ spectral index within the
 804 boundary of the red lines (c) which shows the 2-mm wide sampling range. The red line in (d) indicates the mean index
 805 value and the grey lines represent the one-standard deviations (sd). The colorbar represents the index values of the
 806 distribution map (color figure online). n is the number of rows of the RABD₅₉₀₋₇₆₅ index map.



807

808 **Figure 5: The stratigraphy of total inorganic carbon (TIC), total organic carbon (TOC), sulfur (S) contents, TOC/TN**
 809 **ratio and five phosphorus fractions in sediments of Lake Burgätschi. The y-axis (left) refers to the sediment depth of**
 810 **core Burg17-B. The horizontal red lines separate the significant CONISS zones as in Fig. 3. The secondary y-axis (right)**
 811 **indicates approximate ages of sediments inferred from the Burg17-B core chronology.**

812
 813
 814
 815
 816
 817
 818
 819
 820
 821
 822
 823
 824
 825
 826
 827
 828



829

830

831 **Figure 6: Vertical profile of (a) P fractions concentrations and (b) their proportions of total P in sediments. The y-axis**
 832 **(left) refers to the sediment depth of Core Burg17-B. Note that the sample between 3.6-4.5 cm depth was removed from**
 833 **dataset because the values were extremely higher than any sample data (data not shown), which is abnormal according**
 834 **to XRF-P counts at the corresponding depth (Fig. S8b). We attributed this to the result of contamination during the**
 835 **sample measurements.**

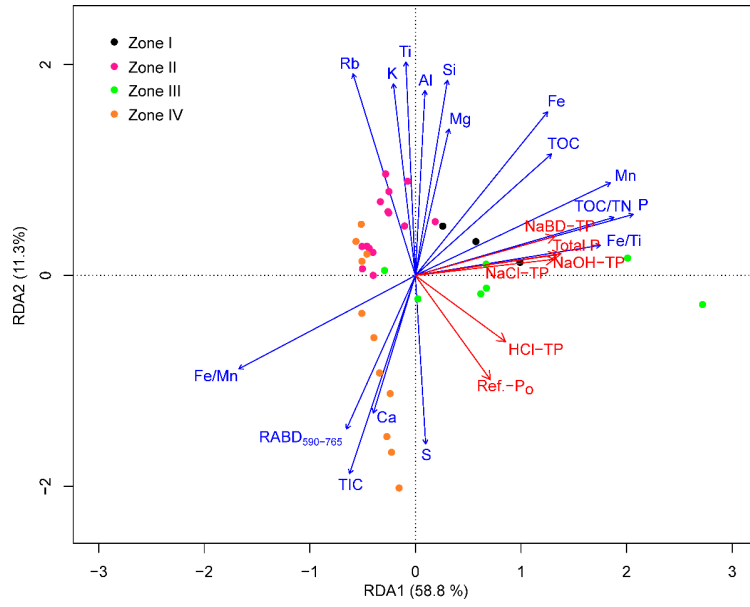
836

837

838

839

840



841
842

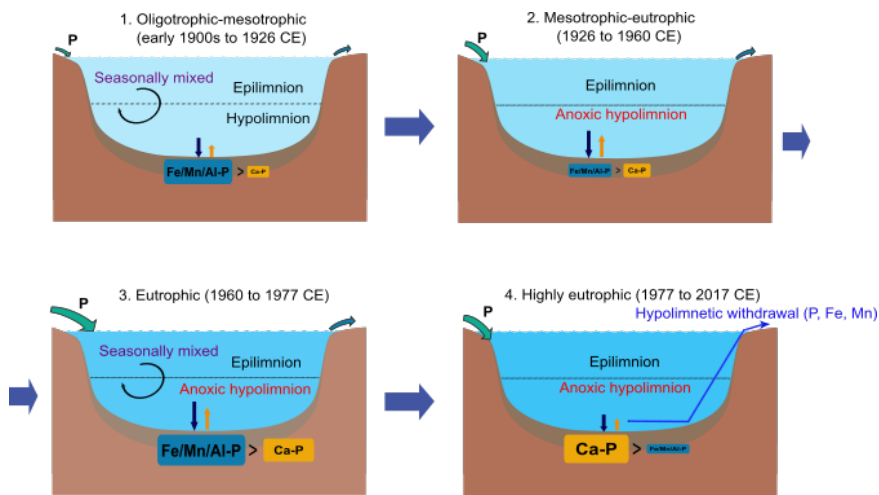
843

844 Figure 7. RDA biplot displaying correlation between response variables (P fraction dataset; red arrows) and
845 explanatory variables (green-pigments and other geochemical records; blue arrows). The colored points represent data
846 points of individual cluster zones in Fig. 3, 5 and S6.

847

848

849



850
851
852
853
854
855
856
857

Figure 8: Conceptual diagram, summarising the inputs/outputs of phosphorus (P), hypolimnetic withdrawal restoration, lake trophic levels, mixing regime and phosphorus (P) fractions retention in sediments of Lake Burgäschi during four stages/zones. Note that the illustrated sizes of P fractions (Fe/Mn/Al-P and Ca-P) among different stages overall indicate the relative amounts of P fractions in sediments.